Pressure-induced electrides and metallic phases in the Y-Cl system

Hulei Yu[1], **Yue Chen**[1,2]‡

[1]Department of Mechanical Engineering, The University of Hong Kong, Pokfulam Road, Hong Kong SAR, China

[2]HKU Zhejiang Institute of Research and Innovation, 1623 Dayuan Road, Lin An 311305, China

E-mail: yuechen@hku.hk

November 2020

Abstract. Pressure can profoundly change the electronic structure, leading to the formation of new phases and materials with exotic properties. Herein, using evolutionary algorithms and density functional theory, we systematically investigate the behaviour of materials in the yttrium-chlorine binary system under pressure. Electrons are found to be spatially confined at low pressures in yttrium chlorides and tend to form new electrides. In particular, a novel yttrium chloride, Y_3Cl_2, is predicted to be thermodynamically and lattice dynamically stable at approximately 10 GPa. Further analyses of the electron localization function and partial charge density identify trigonal Y_3Cl_2 as a new 2D high-pressure electride (HPE) with partially localized electrons contributing to the conduction. By further increasing the pressure, electrons in the yttrium-chlorine binary system tend to delocalize with the electrides decomposing into two new compounds (Y_2Cl and YCl_2) and a new YCl phase (space group $P6_3/mmc$) above 20 GPa. These newly discovered phases are all metallic in their stable pressure range according to band structure simulations without interstitial electron localization. The discovery of these unconventional yttrium chlorides may inspire strategies to search for low-pressure electrides in other rare-earth halogenide systems.

Keywords: evolutionary algorithm, electride, high-pressure, first-principles, Y-Cl
Submitted to: *J. Phys.: Condens. Matter*

‡ Author to whom any correspondence should be addressed.

1. Introduction

Electrides are a class of peculiar materials with spatially trapped excess electrons serving as anions.[1, 2] Induced by the particular electron states in electrides, the unusual chemical, electronic or optical performances enable various applications as catalysts[3, 4], battery anodes[5], or electron-injection barrier materials.[6] Compared with organic electrides, inorganic electrides are expected to exhibit better stability and superior capabilities [7, 8].

Since the synthesis of the first room-temperature-stable inorganic electride $Ca_{24}Al_{28}O_{64}$,[9] only a handful of inorganic electrides have been found under ambient conditions (*e.g.*, Y_5Si_3[4], Ca_2N[10], Y_2C[11], Sr_3CrN_3[12]). As the bonding patterns and stability of materials can be significantly changed by compression, unexpected phases and crystal structures that are inaccessible under ambient conditions with intriguing properties may be obtained.[13, 14, 15] Pressure application has also become an effective approach in research on exploring electrides. On the basis of theory-assisted material predictions, a variety of novel high-pressure electrides (HPEs) have been identified. Accompanied by a metal-insulator transition, an optically transparent dense sodium phase was found by Ma et al. at approximately 200 GPa.[16] This insulating Na phase was categorized as a canonical 0D electride due to the formation of localized interstitial electron pairs (interstitial quasiatoms).[16, 17] Similar 0D HPEs were also observed in some pressurized elemental phases, *e.g.*, Li,[18, 19] K,[20] Ca,[21] and Al[22]. In some other elements such as thallium[23], HPEs were absent even at terapascal pressures. Pressure-induced phase transitions between 2D electrides and 0D HPEs were found in alkaline-earth-metal subnitrides (Ca_2N, Sr_2N and Ba_2N) in both theoretical structural searches and high-pressure synchrotron experiments.[24] Some HPEs were induced by the formation of unexpected cation-rich compounds. Dong et al. theoretically predicted the existence of a 0D HPE with the formation of a thermodynamically stable compound between Na and inert He (Na_2He), and this compound was later confirmed in an experimental synthesis.[25] High-temperature superconducting HPEs were also experimentally realized in pressure-stabilized Li-rich phosphides with unconventional stoichiometries (*e.g.*, Li_6P, Li_5P, $Li_{11}P_2$).[26]

Yttrium chlorides, as important halides, have attracted much attention in electride research. The most common compound in the Y-Cl binary system is YCl_3. This colourless solid crystallizes in a monoclinic structure (space group $C2/m$, Pearson symbol mS16) under ambient conditions and is widely applied as an additive for batteries[27] or as a Lewis acid for reactions[28]. The two other compounds in the Y-Cl binary system observed under ambient conditions are Y_2Cl_3 and YCl[29], which belong to a new class of electrides[30]. Y_2Cl_3 possesses a monoclinic structure (space group $C2/m$, Pearson symbol mS20) with a prototype of Gd_2Cl_3. In contrast to insulating YCl_3[31], Y_2Cl_3 is a semiconductor with an indirect bandgap of 1.14 eV.[30] Electron localization is found in the channel-like voids in Y_2Cl_3, and the confined electrons are weakly bonded with each other, making Y_2Cl_3 a quasi-1D electride.[32, 30] Similar

to typical Ca_2N-type 2D electrides,[33] YCl also adopts a laminar structure in the $R\bar{3}m$ space group. Nonetheless, anionic electrons are observed between every two Y-Cl layers instead of in all interlayer spaces.[30] Therefore, YCl was identified as a quasi-2D electride.[30] In addition, the Y in these reduced rare-earth halides adopts an oxidation state of +2 rather than the more common oxidation state of +3[34], quantifying these two electrides as $[YCl]^+ \cdot e^-$ and $[Y_2Cl_3]^+ \cdot e^-$.[30]

Despite the study of Y-Cl compounds at ambient pressure, the behaviour of the Y-Cl system under pressure is largely unexplored. Here, we have systematically investigated the Y-Cl binary systems under hydrostatic pressures up to 60 GPa based on first-principles structural searches with evolutionary algorithms. Novel pressure-induced stable and metastable phases in the Y-Cl binary system are predicted, and the related electronic properties are studied. Localized electrons under pressure are observed in the Y-Cl system with the formation of a new stable HPE and several potential metastable HPEs. At higher pressures, the HPEs are predicted to spontaneously decompose into energetically preferable phases, which have unconventional stoichiometries and exist in a large pressure range.

2. Computational methods

Evolutionary algorithm-based crystal structure predictions within the framework of density functional theory (DFT) under pressure were performed using USPEX [35] interfaced with the Vienna ab initio simulation package (VASP) [36]. The maximum number of atoms in a randomly generated unit cell was set to 18. The crystal structures of all compounds in the Y-Cl system available in the Materials Project database [31] were taken into account as seeds in the search.[37] The first generation consisted of 50 randomly generated crystal structures and seeds. Each subsequent generation with 40 new crystal structures was generated by heredity (40%), random (20%), softmutation/coormutation (20%), and transmutation (20%). The structural searches were stopped as the best structures remained unchanged for 20 generations. The projector-augmented wave (PAW) method [38] was applied with the generalized gradient approximation (GGA) of Perdew-Burke-Ernzerhof (PBE) [39]. All crystal structures were relaxed into their ground states by calculating the atomic forces and the full stress tensor. The Γ-centred Monkhorst-Pack method [40] at a grid spacing of approximately $0.03 \times 2\pi$ Å^{-1} was used in meshing Brillouin zones. A plane-wave energy cut-off of 340 eV was applied in all DFT computations, and the convergence criterion for electronic self-consistent calculations was set to 10^{-6} eV. Supercells ($3 \times 3 \times 3$ with 135 atoms for Y_3Cl_2, $3 \times 3 \times 3$ with 162 atoms for Y_2Cl, $4 \times 4 \times 2$ with 128 atoms for YCl, and $4 \times 4 \times 4$ with 192 atoms for YCl_2) were adopted to study the phonon properties using the small displacement method [41]. To ensure the accuracy of phonon dispersions, a more stringent total energy convergence criterion of 10^{-8} eV was used.

3. Results and discussion

No energetically preferable compound with Cl/(Y+Cl) > 0.75 is found in our structural searches up to the maximum pressure (60 GPa) we consider in this work. Thus, the enthalpies of formation in Fig. 1 are computed with respect to the most stable Y and YCl_3 phases at each selected pressure. It is seen from the convex hulls in Fig. 1 that the experimentally observed YCl ($R\bar{3}m$, hR12), Y_2Cl_3 ($C2/m$, mS20) and YCl_3 ($C2/m$, mS16) are all reproduced as the lowest-energy phases at 0 GPa, indicating the reliability of our predictions. It is worth noting that our calculations suggest that Y_2Cl_3 and YCl_3 are thermodynamically stable, while YCl is metastable (above the convex hull) at 0 GPa. Localized electrons are observed in the YCl and Y_2Cl_3 electrides at 0 GPa based on the calculations of the electron localization function (ELF) (see Fig. S1 in the Supporting Information), which is consistent with previous research[30].

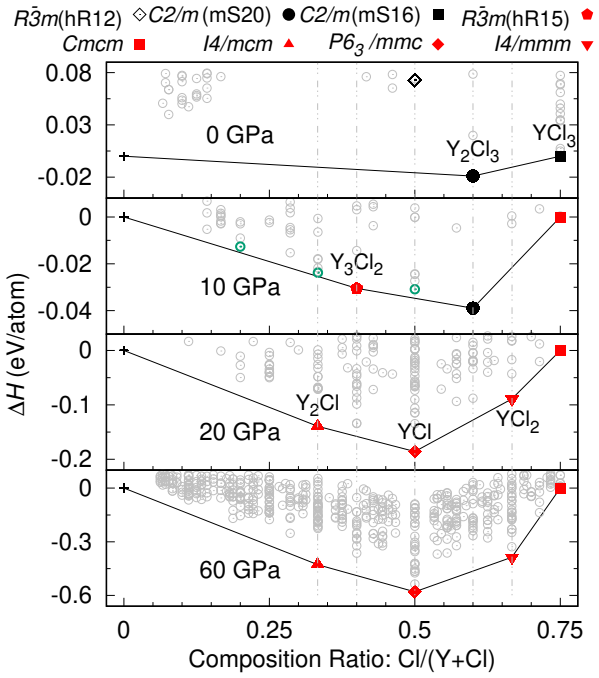

Figure 1. Stability of predicted yttrium chlorides at various pressures. Gray and green circles represent high-energy crystal structures and potential metastable HPEs, respectively.

By exerting a hydrostatic pressure of 10 GPa, no structural phase transition is found in the quasi-2D electride Y_2Cl_3. On the other hand, YCl_3 is predicted to undergo a phase transition into an orthorhombic structure with the $Cmcm$ space group at 10 GPa. In addition to these two long-known compounds, a novel compound with a counterintuitive Y:Cl stoichiometry of 3:2 becomes energetically favourable at 10 GPa. It has a trigonal crystal structure in the $R\bar{3}m$ space group with layered Y-Cl-Y-Cl-Y stacking. Detailed structural information of the predicted phases is summarized in Table S1 in the Supporting Information. In addition to the thermodynamic stability,

the lattice dynamic stabilities of the Y_3Cl_2 compound and the new YCl_3 phase are also studied. As displayed in Fig. S2 in the Supporting Information, no imaginary phonon mode is observed at either 10 GPa or 0 GPa, indicating that *Cmcm*-YCl_3 and Y_3Cl_2 are dynamically stable at both 10 GPa and 0 GPa. Thus, high-pressure *Cmcm*-YCl_3 and Y_3Cl_2 may be quenchable to ambient conditions.

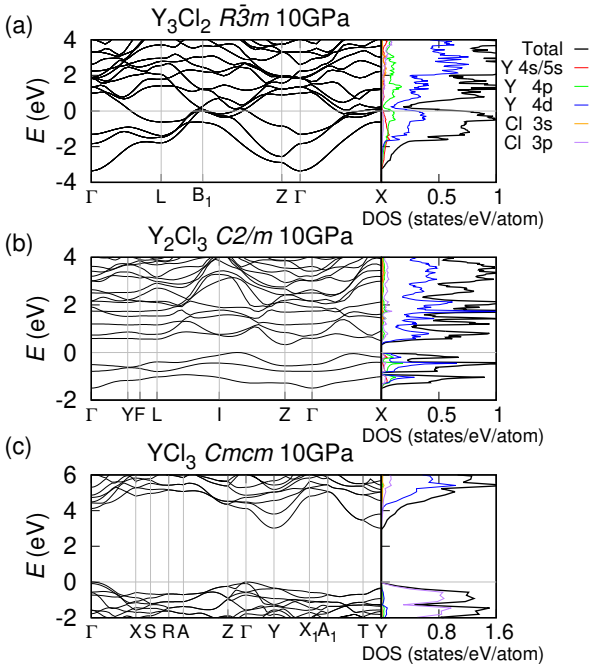

Figure 2. Electronic band structures and projected density of states of predicted stable yttrium chlorides at 10 GPa. Fermi levels are shifted to 0 eV.

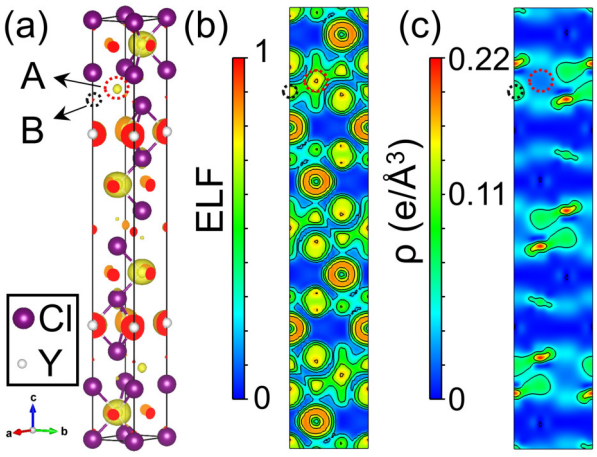

Figure 3. (a) Electron localization function of Y_3Cl_2 at 10 GPa. The isosurface is set at a value of 0.75. Y and Cl atoms are coloured purple and white, respectively. (b) ELF contours of Y_3Cl_2 on the (110) plane. (c) Partial charge density distribution ($\pm$0.05 eV from E_f) of Y_3Cl_2 on the (110) plane. The positions of different ELF attractors (non-nuclear ELF maxima) are highlighted by red and black dashed circles.

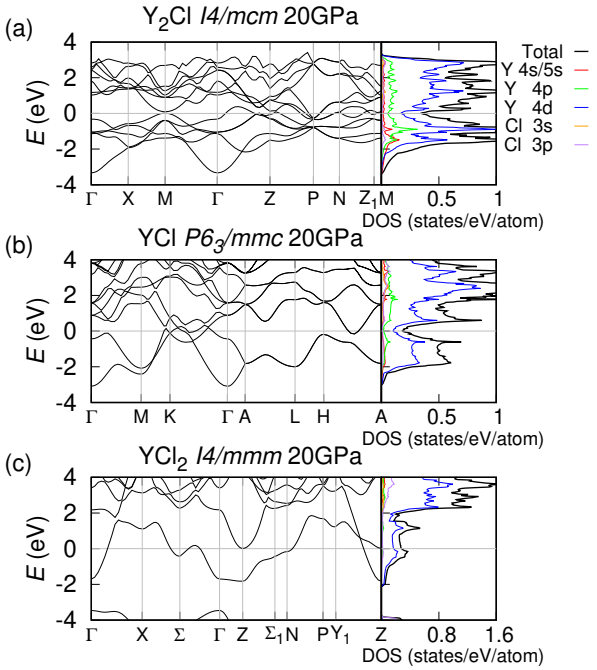

Figure 4. Electronic band structures and projected density of states of predicted stable yttrium chlorides at 20 GPa. Fermi levels are shifted to 0 eV.

Fig. 2 presents the computed electronic band structures and projected density of states (DOS) of the predicted stable compounds at 10 GPa. Significant differences in the electronic structures among these three compounds are noted. Similar to the insulated $C2/m$ phase of YCl_3 under ambient conditions, the pressure-induced $Cmcm$ phase is also found to be an insulator with a large indirect bandgap of approximately 3.02 eV at 10 GPa. The conduction band minimum (CBM) and the valence band maximum (VBM) are located at the Y and Γ points, respectively. The bottom of the conduction bands are mainly contributed by the Y *4d* states; the top of the valance bands largely originate from the Cl *3p* states. For Y_2Cl_3 under a hydrostatic pressure of 10 GPa, it remains semiconducting with a small indirect bandgap of approximately 0.33 eV. In contrast to the $C2/m$ phase of YCl_3, the Y *4p* and *4d* orbitals contribute the dominant parts of the DOS around the VBM of Y_2Cl_3. Particularly, a metallic character is found in Y_3Cl_2, as electronic bands cross the Fermi level (E_F). The most significant contribution to the DOS in the vicinity of E_F is found to originate from the Y *4d* orbitals.

The Bader charges of Y and Cl in $Cmcm$-YCl_3 are found to be +2.06 and -0.68, respectively. Therefore, strong ionic bonds are expected, and the valence states in $Cmcm$-YCl_3 at 10 GPa are +3 and -1 for Y and Cl, respectively, rationalizing the insulation state of $Cmcm$-YCl_3. On the other hand, the Bader charges of Y are found to be +0.86/+1.41 in Y_2Cl_3, suggesting a lower oxidation state of +2, consistent with the previously proposed formula of $[Y_2Cl_3]^+ \cdot e^-$ [30]. The extra electron localizes in space, leading to the semiconducting state of Y_2Cl_3 at 10 GPa. Even lower Bader charges (+0.45/+0.98) are predicted for Y in Y_3Cl_2, suggesting an oxidation state of

+1 and a formula of $[Y_3Cl_2]^+ \cdot e^-$. As will be discussed in the following, although Y_3Cl_2 is predicted to be an electride at 10 GPa, the electron localization may not be strong enough to produce an insulating state.

The ELF and partial charge density are further calculated to analyse the electride characteristics of Y_3Cl_2. As depicted in Fig. 3 (a-b), two different kinds of ELF attractors (ELF maxima off the nuclei) can be observed between two adjacent Y-Cl-Y-Cl-Y layers, indicating that Y_3Cl_2 is a 2D HPE. Similar to the attractors in $R\bar{3}m$-YCl and Y_2Cl_3[30], these attractors are connected to delocalized electrons throughout the interlayer interstitial spaces. Moreover, the confined electrons are more localized at attractor A sites than at B sites, with a higher maximum ELF value. The partial electron density corresponding to the region near the Fermi energy (Fig. 3 (c)) suggests that the excess electrons near the attractor A sites do not demonstrate conducting behaviour, whereas the electrons near B sites contribute to the electronic transport of the system. In contrast, the energies of the localized electrons in quasi-1D HPE Y_2Cl_3 are all below the Fermi level [30], leading to a semiconductor instead of a metal. In addition to Y_3Cl_2 and Y_2Cl_3, a few other potentially metastable yttrium chlorides at 10 GPa (the low-energy phases near the convex hull in Fig. 1) are also predicted to be HPEs (see the Supporting Information), implying the tendency for interstitial electron localization in the Y-Cl system at 10 GPa.

By further compressing the Y-Cl binary system, we find more unexpected compounds to be stable. Four energetically preferable compounds (Y_2Cl, YCl, YCl_2 and YCl_3) are predicted on the convex hulls in Fig. 1 at 20 GPa. All these compounds remain energetically favourable up to 60 GPa without any structural phase transition. The large pressure range where these four compounds are predicted to be stable suggests that they are more likely to be synthesized in experiments. The chemically counterintuitive tetragonal compounds Y_2Cl and YCl_2 possess space groups of $I4/mcm$ and $I4/mmm$, respectively. The newly discovered YCl high-pressure phase has a hexagonal crystal structure with the $P6_3/mmc$ space group. Unlike the previously known metastable $R\bar{3}m$ phase under ambient conditions, $P6_3/mmc$ is an energetically stable phase. Moreover, the disappearance of Y_3Cl_2 and Y_2Cl_3 on the convex hull at 20 GPa implies their potential spontaneous decomposition at this pressure. Based on the calculated phonon dispersions (shown in Fig. S6 in the Supporting Information), it is notable that large imaginary vibrational frequencies exist in Y_2Cl at 0 GPa, whereas no imaginary phonon mode is found for Y_2Cl at 20 GPa. Therefore, Y_2Cl is lattice dynamically stable only under pressure. In contrast, $P6_3/mmc$-YCl and YCl_2 are lattice dynamically stable at both high pressure and 0 GPa, suggesting that they may be quenchable to ambient conditions.

As the pressure increases to 20 GPa, the electronic properties of the compounds are also significantly altered. From the gapless electronic band structures shown in Fig. 4, $P6_3/mmc$-YCl, Y_2Cl and YCl_2 are all metallic at 20 GPa. From the projected DOS shown in Fig. 4 (a), the Y *4p* and *4d* orbitals contribute most to the DOS of Y_2Cl near the Fermi level. In contrast, the metallization of $P6_3/mmc$-YCl and YCl_2

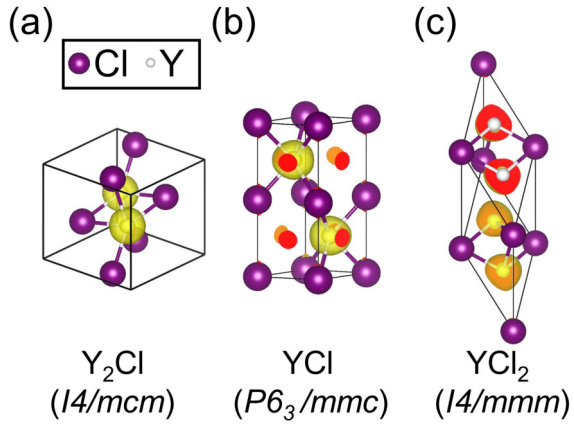

Figure 5. Electron localization function of predicted stable yttrium chlorides Y_2Cl (a), YCl (b) and YCl_2 (c) at 20 GPa. The isosurfaces are set at a value of 0.75. Y and Cl atoms are coloured purple and white, respectively.

mainly originates from Y *4d* orbitals. Bader charge analysis at 20 GPa also shows an increase in the electron donation of Y atoms as the ratio of Y in compounds decreases (the Bader charges of Y are +0.50, +0.94, +1.52 and +2.03 in Y_2Cl, $P6_3/mmc$-YCl, YCl_2 and $Cmcm$-YCl_3, respectively), implying an enhancement of the ionic bonding character in compounds with a higher Cl ratio. In addition, none of these high-pressure compounds are HPEs, as no obvious spatially confined electrons are found from their ELFs, as shown in Fig. 5. Therefore, a higher pressure tends to delocalize electrons in the Y-Cl system.

4. Conclusions

The Y-Cl binary system is systematically investigated under hydrostatic pressures up to 60 GPa based on first-principles structural searches with evolutionary algorithms. Novel stable and metastable yttrium chlorides are predicted from our computations. In particular, trigonal Y_3Cl_2 is found to be energetically and lattice dynamically stable at approximately 10 GPa. The confined excess electrons between two adjacent yttrium layers, which partially contribute to the electrical transport, suggest that Y_3Cl_2 is a 2D HPE. Above 20 GPa, the electrides are predicted to simultaneously decompose into Y_2Cl, YCl, and YCl_2 compounds, which are all metallic above 20 GPa. Therefore, as pressure increases, electrons in the Y-Cl binary system first become localized with the formation of new HPEs and then become more delocalized with the formation of new metallic phases. Our results provide guidance on the discovery of new HPEs in other rare-earth halide systems.

Acknowledgments

This work is supported by the Research Grants Council of Hong Kong (17300018 and 17201019), the National Natural Science Foundation of China (51706192 and 11874313), the Zhejiang Provincial Natural Science Foundation (LR19A040001), and the Environment and Conservation Fund (69/2018). The authors are grateful for the research computing facilities offered by ITS, HKU.

References

[1] James L. Dye. Electrons as anions. *Science*, 301(5633):607–608, 2003.

[2] Mao-Sheng Miao and Roald Hoffmann. High pressure electrides: A predictive chemical and physical theory. *Acc. Chem. Res.*, 47(4):1311–1317, 2014.

[3] Masaaki Kitano, Shinji Kanbara, Yasunori Inoue, Navaratnarajah Kuganathan, Peter V Sushko, Toshiharu Yokoyama, Michikazu Hara, and Hideo Hosono. Electride support boosts nitrogen dissociation over ruthenium catalyst and shifts the bottleneck in ammonia synthesis. *Nat. Commun.*, 6(1):1–9, 2015.

[4] Yangfan Lu, Jiang Li, Tomofumi Tada, Yoshitake Toda, Shigenori Ueda, Toshiharu Yokoyama, Masaaki Kitano, and Hideo Hosono. Water durable electride y5si3: Electronic structure and catalytic activity for ammonia synthesis. *J. Am. Chem. Soc.*, 138(12):3970–3973, 2016.

[5] Junping Hu, Bo Xu, Shengyuan A. Yang, Shan Guan, Chuying Ouyang, and Yugui Yao. 2d electrides as promising anode materials for na-ion batteries from first-principles study. *ACS Appl. Mater.*, 7(43):24016–24022, 2015.

[6] Hideo Hosono, Junghwan Kim, Yoshitake Toda, Toshio Kamiya, and Satoru Watanabe. Transparent amorphous oxide semiconductors for organic electronics: Application to inverted oleds. *Proc. Natl. Acad. Sci. U.S.A*, 114(2):233–238, 2017.

[7] Motoaki Hirayama, Satoru Matsuishi, Hideo Hosono, and Shuichi Murakami. Electrides as a new platform of topological materials. *Phys. Rev. X*, 8:031067, Sep 2018.

[8] Qiang Zhu, Timofey Frolov, and Kamal Choudhary. Computational discovery of inorganic electrides from an automated screening. *Matter*, 1(5):1293 – 1303, 2019.

[9] Satoru Matsuishi, Yoshitake Toda, Masashi Miyakawa, Katsuro Hayashi, Toshio Kamiya, Masahiro Hirano, Isao Tanaka, and Hideo Hosono. High-density electron anions in a nanoporous single crystal: [ca24al28o64]4+(4e-). *Science*, 301(5633):626–629, 2003.

[10] Kimoon Lee, Sung Wng Kim, Yoshitake Toda, Satoru Matsuishi, and Hideo Hosono. Dicalcium nitride as a two-dimensional electride with an anionic electron layer. *Nature*, 494(7437):336–340, 2013.

[11] Huaqing Huang, Kyung-Hwan Jin, Shunhong Zhang, and Feng Liu. Topological electride y2c. *Nano Lett.*, 18(3):1972–1977, 2018.

[12] Padtaraporn Chanhom, Kevin E. Fritz, Lee A. Burton, Jan Kloppenburg, Yaroslav Filinchuk, Anatoliy Senyshyn, Maoyu Wang, Zhenxing Feng, Numpon Insin, Jin Suntivich, and Geoffroy Hautier. Sr3crn3: A new electride with a partially filled d-shell transition metal. *J. Am. Chem. Soc.*, 141(27):10595–10598, 2019.

[13] Hulei Yu, Xiaohuan Lin, Kuo Li, and Yue Chen. Unveiling a novel, cation-rich compound in a high-pressure pb–te binary system. *ACS Cent. Sci.*, 5(4):683–687, 2019.

[14] Jianjun Mao and Yue Chen. Ground-state crystal structures of superconducting nb3al and the phase transformation under high pressures. *J. Appl. Phys.*, 124(17):173902, 2018.

[15] Hulei Yu, Dexiang Gao, Xiancheng Wang, Xueyan Du, Xiaohuan Lin, Wenhan Guo, Ruqiang Zou, Changqing Jin, Kuo Li, and Yue Chen. Unraveling a novel ferroelectric gese phase and its transformation into a topological crystalline insulator under high pressure. *NPG Asia Mater.*, page 1, 2018.

[16] Yanming Ma, Mikhail Eremets, Artem R Oganov, Yu Xie, Ivan Trojan, Sergey Medvedev, Andriy O Lyakhov, Mario Valle, and Vitali Prakapenka. Transparent dense sodium. *Nature*, 458(7235):182–185, 2009.

[17] Yinwei Li, Yanchao Wang, Chris J. Pickard, Richard J. Needs, Yi Wang, and Yanming Ma. Metallic icosahedron phase of sodium at terapascal pressures. *Phys. Rev. Lett.*, 114:125501, Mar 2015.

[18] Takahiro Matsuoka and Katsuya Shimizu. Direct observation of a pressure-induced metal-to-semiconductor transition in lithium. *Nature*, 458(7235):186–189, 2009.

[19] Jian Lv, Yanchao Wang, Li Zhu, and Yanming Ma. Predicted novel high-pressure phases of lithium. *Phys. Rev. Lett.*, 106:015503, Jan 2011.

[20] Chris J. Pickard and R. J. Needs. Predicted pressure-induced *s*-band ferromagnetism in alkali metals. *Phys. Rev. Lett.*, 107:087201, Aug 2011.

[21] Artem R. Oganov, Yanming Ma, Ying Xu, Ion Errea, Aitor Bergara, and Andriy O. Lyakhov. Exotic behavior and crystal structures of calcium under pressure. *Proc. Natl. Acad. Sci. U.S.A*, 107(17):7646–7651, 2010.

[22] Chris J Pickard and RJ Needs. Aluminium at terapascal pressures. *Nat. Mater.*, 9(8):624–627, 2010.

[23] C Cazorla, S G MacLeod, D Errandonea, K A Munro, M I McMahon, and C Popescu. Thallium under extreme compression. *J. Phys. Condens. Matter*, 28(44):445401, sep 2016.

[24] Yunwei Zhang, Weikang Wu, Yanchao Wang, Shengyuan A. Yang, and Yanming Ma. Pressure-stabilized semiconducting electrides in alkaline-earth-metal subnitrides. *J. Am. Chem. Soc.*, 139(39):13798–13803, 2017.

[25] Xiao Dong, Artem R Oganov, Alexander F Goncharov, Elissaios Stavrou, Sergey Lobanov, Gabriele Saleh, Guang-Rui Qian, Qiang Zhu, Carlo Gatti, Volker L. Deringer, Richard Dronskowski, Xiang-Feng Zhou, Vitali B. Prakapenka, Zuzana Konpkov, Ivan A. Popov, Alexander I. Boldyrev, and Hui-Tian Wang. A stable compound of helium and sodium at high pressure. *Nat. Chem.*, 9(5):440–445, 2017.

[26] Ziyuan Zhao, Shoutao Zhang, Tong Yu, Haiyang Xu, Aitor Bergara, and Guochun Yang. Predicted pressure-induced superconducting transition in electride li_6P. *Phys. Rev. Lett.*, 122:097002, Mar 2019.

[27] Yan Xu, Guangmin Zhou, Shuyang Zhao, Wanfei Li, Feifei Shi, Jia Li, Jun Feng, Yuxing Zhao, Yang Wu, Jinghua Guo, Yi Cui, and Yuegang Zhang. Improving a mg/s battery with ycl3 additive and magnesium polysulfide. *Adv. Sci.*, 6(4):1800981, 2019.

[28] Ounjit Sodpiban, Silvano Del Gobbo, Samir Barman, Vatcharaporn Aomchad, Pinit Kidkhunthod, Samy Ould-Chikh, Albert Poater, Valerio D'Elia, and Jean-Marie Basset. Synthesis of well-defined yttrium-based lewis acids by capturing a reaction intermediate and catalytic application for cycloaddition of co2 to epoxides under atmospheric pressure. *Catal. Sci. Technol.*, 9:6152–6165, 2019.

[29] H. Mattausch, J. B. Hendricks, R. Eger, J. D. Corbett, and A. Simon. Reduced halides of yttrium with strong metal-metal bonding: Yttrium monochloride, monobromide, sesquichloride, and sesquibromide. *Inorg. Chem.*, 19(7):2128–2132, 1980.

[30] Biao Wan, Yangfan Lu, Zewen Xiao, Yoshinori Muraba, Junghwan Kim, Dajian Huang, Lailei Wu, Huiyang Gou, Jingwu Zhang, Faming Gao, Ho-kwang Mao, and Hideo Hosono. Identifying quasi-2d and 1d electrides in yttrium and scandium chlorides via geometrical identification. *Npj Comput. Mater.*, 4(1):1–9, 2018.

[31] Anubhav Jain, Shyue Ping Ong, Geoffroy Hautier, Wei Chen, William Davidson Richards, Stephen Dacek, Shreyas Cholia, Dan Gunter, David Skinner, Gerbrand Ceder, and Kristin a. Persson. Commentary: The Materials Project: A Materials Genome Approach to Accelerating Materials Innovation. *APL Mater.*, 1(1):011002, 2013.

[32] Kyeong Ae Yee and Timothy Hughbanks. Semilocalized bonding schemes in extended systems; orbital localization in yttrium chloride (y2cl3) and interstitial derivatives. *Inorg. Chem.*,

31(9):1620–1625, 1992.

[33] Yunwei Zhang, Hui Wang, Yanchao Wang, Lijun Zhang, and Yanming Ma. Computer-assisted inverse design of inorganic electrides. *Phys. Rev. X*, 7:011017, Feb 2017.

[34] Gerd Meyer and H Juergen Meyer. Unusual valences in rare-earth halides. *Chem. Mater.*, 4(6):1157–1168, 1992.

[35] Lyakhov Andriy O., Oganov Artem R., and Valle Mario. *Crystal Structure Prediction Using Evolutionary Approach*, chapter 7, pages 147–180. Wiley-Blackwell, Weinheim, 2010.

[36] Georg Kresse and Jürgen Furthmüller. Efficiency of ab-initio total energy calculations for metals and semiconductors using a plane-wave basis set. *Comput. Mater. Sci.*, 6(1):15–50, 1996.

[37] Artem R Oganov, Andriy O Lyakhov, and Mario Valle. How evolutionary crystal structure prediction worksand why. *Acc. Chem. Res.*, 44(3):227–237, 2011.

[38] Peter E Blöchl. Projector augmented-wave method. *Phys. Rev. B*, 50(24):17953, 1994.

[39] John P Perdew, Kieron Burke, and Matthias Ernzerhof. Generalized gradient approximation made simple. *Phys. Rev. Lett.*, 77(18):3865, 1996.

[40] Hendrik J Monkhorst and James D Pack. Special points for brillouin-zone integrations. *Phys. Rev. B*, 13(12):5188, 1976.

[41] A Togo and I Tanaka. First principles phonon calculations in materials science. *Scr. Mater.*, 108:1–5, Nov 2015.